

Toward the design of a very cold neutron source for the High Brilliance Source

D.D. Maharaj , U. Rücker, J. Li, J. Voigt, T. Gutberlet, and P. Zakalek 

Jülich Centre for Neutron Science, Forschungszentrum Jülich, Wilhelm-Johnen-Straße, Jülich 52425, Germany

Corresponding author: D.D. Maharaj (email: maharaj.dalini@gmail.com)

Abstract

In contrast to the moderator designs typical of large reactor and spallation sources, high-current accelerator-driven neutron sources, with smaller source dimensions, necessitate highly efficient and compact moderator solutions. At the High Brilliance Source (HBS), a hydrogen-rich moderator is required to effectively slow neutrons to the very cold neutron (VCN) energy range within the limited volume that aligns with the HBS target size. Methane, a well-established and highly efficient neutron moderator is a promising candidate to serve as a VCN moderator since it possesses a desirable low-lying rotor mode at ~ 1 meV to facilitate neutron slowing. Liquid parahydrogen (pH_2) is a known efficient cold neutron moderator since it is able to convert thermal neutrons to cold neutrons via a single interaction. A geometrical configuration combining methane, embedded in pH_2 has been investigated to harness the complementary properties of both materials as a potential VCN moderator design for the HBS. Monte Carlo simulations using the Particle and Heavy Ion Transport code System particle transport code were conducted to evaluate the performance of the combined moderator concept when compared with a pure, low-dimensional pH_2 cold source.

Key words: very cold neutrons, neutron sources, Monte Carlo methods

1. Introduction

Very cold neutrons (VCNs) are defined over a wide spectral range, from 1 meV (9 \AA) down to a few 100 neV ($> \text{several } 100 \text{ \AA}$). They provide an unprecedented opportunity for neutron scientists to probe structures on the nanoscale, and dynamics on extended time scales in neutron scattering experiments [1]. For this reason, it has been of great interest to the global neutron community to develop VCN sources over the last 20 years [2–4]. At a workshop held at Argonne National Laboratory in 2005, two key challenges were identified in the realisation of VCN moderators. Sufficiently high intensities of VCNs were not achievable hitherto at pre-existing neutron sources because the Maxwellian spectra produced by conventional cold moderators generate insufficient neutron intensities in the very cold energy spectrum since the neutron intensity falls off with neutron wavelength, λ , as $1/\lambda^5$. Secondly, the lack of thermal scattering cross sections for potential new VCN moderator materials precluded the conceptual study of VCN moderators with the use of Monte Carlo particle transport techniques [2].

The development of VCN sources at spallation neutron facilities including the Second Target Station at Oak Ridge National Laboratory and the European Spallation Source (ESS) remains to be a top research priority to expand the scientific capabilities of neutron scattering techniques [3–5]. In the context of high-current accelerator-driven neutron sources (HiCANS), the High Brilliance Source (HBS) stands out as a par-

ticularly promising candidate for realising a VCN source. This is primarily due to its planned capability to deliver pulsed proton beams with a high peak power of 100 kW to a tantalum target [6]. As a HiCANS facility, the HBS offers several advantages over spallation sources for VCN production. Spallation sources typically generate higher radiation fields, which prevent the use of the highly efficient VCN moderator candidate material, methane, because it undergoes radiolysis under such conditions [7]. Additionally, spallation sources impose significantly larger heat loads on moderator systems, and this demands careful consideration of the placement and design of VCN moderator systems. The conceptual designs developed for the VCN moderator system for the ESS rely on the implementation of solid deuterium ($s\text{-D}_2$) and deuterated clathrate hydrates containing molecular O_2 , which require very low operating temperatures of 5 and 2.4 K, respectively [4]. To maintain these operating conditions, the VCN moderators at spallation sources must consequently be positioned further from the target, which reduces the coupling between the primary neutron source and the moderator. By contrast, HiCANS facilities like the HBS allow moderator systems to be placed much closer to the target, improving the coupling between the source and the moderator and enhancing neutron production efficiency. Furthermore, the lower radiation and thermal loads at HiCANS relax the performance requirements for cryogenic VCN moderator systems, making their design and operation considerably more feasible.

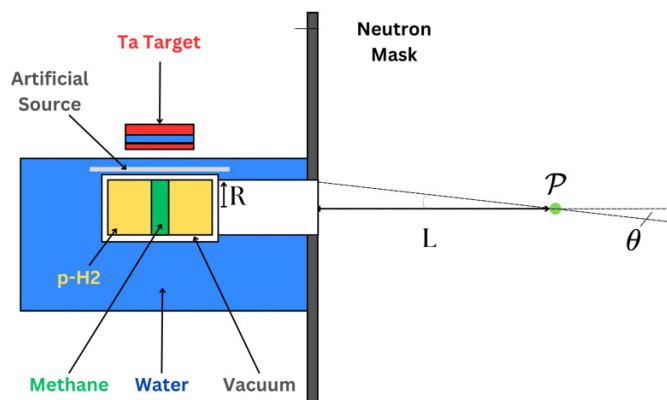
When selecting an appropriate VCN moderator material for the HBS, it is essential to consider that HiCANS are designed on the principle that there is strong coupling between neutrons generated at the primary source (target), the moderator-reflector systems, and the neutron scattering instruments. Therefore, the VCN moderator must be capable of efficiently moderating neutrons within a compact moderator volume, which is typically constrained by the footprint of the neutron generation target. While a VCN moderator concept based on s-D₂ is a viable solution at the ESS, it is not at HiCANS because its weak total scattering cross section for thermal neutrons implies that a large volume of s-D₂ will be required to moderate the neutrons to VCN energies, and will result in deconfinement of the neutron cloud coming from the primary source and premoderator.

An ideal VCN moderator for the HBS would be a hydrogen-rich material that possesses a strong total scattering cross section. As the single-phonon contribution to the neutron cross section falls off as $\sim \left(\frac{T}{k_B \Theta_D}\right)^3$, and drops off increasingly faster for higher-order processes, where Θ_D is the Debye temperature of the lattice, k_B is the Boltzmann constant [8], a VCN candidate material must possess vacant low-lying energy states on the scale of a few \sim meV, which are not constrained by a dispersion relation. Methane is a well-established material which matches these requirements. Below 20.4 K, solid methane has a face-centred cubic crystal structure and is said to enter phase II in which only a 1/4 of the molecules at the crystallographic O_h sites act as free rotors [9]. The free rotor mode has an inelastic excitation energy of \sim 1 meV and provides a mechanism for neutron cooling [9].

This study represents a first step toward the effort to realise a VCN source at the HBS. Already, a low-dimensional cold parahydrogen (pH₂) moderator has been designed and tested for the HBS and it is known to produce high brilliance, cold neutron beams [6]. It is classified as a low-dimensional moderator as a result of the comparably larger dimension of the moderator along the extraction direction versus the dimension along which the moderator is fed with thermal neutrons. The confluence of two unique nuclear properties of pH₂, namely, the efficient conversion of thermal neutrons to cold neutrons within a single interaction over 1 cm, alongside the long path length for cold neutrons, of 10 cm in pH₂, underscores the low-dimensional moderator concept. Methane, as a VCN moderator candidate, generates a colder neutron spectrum when compared with pH₂ [10].

The objective of this study is to determine whether it is possible to leverage the strengths of pH₂ as a brilliant source of cold neutrons to feed a volume of methane moderator, which would be employed as a VCN converter medium. When conceiving the VCN moderator concept, absorption effects should also be considered since the rate of neutron absorption is proportional to $1/v$, where v is the neutron velocity. Absorption is more pronounced for cold neutrons in methane than in pH₂ as a consequence of the comparably shorter path length for cold neutrons, which implies the higher likelihood of a scattering or absorption event. Therefore, the moderator dimensions and geometry need to be selected wisely, to strike

Fig. 1. Illustration of the geometrical concept for evaluating the quantity \mathcal{B} , which is the flux Φ per unit solid angle where Φ is obtained from the point tally estimate in Particle and Heavy Ion Transport code System.



the balance between ensuring proper neutron moderation, while minimising neutron absorption.

2. Methods

For this study, simulations are performed with the general purpose Monte Carlo particle transport simulation code, Particle and Heavy Ion Transport code System (PHITS) [11, 12] to evaluate the performance of the moderator concept presented in Fig. 1. This investigation is conducted in two stages. First, the geometrical parameters defining the combined moderator geometry, which is presented in Fig. 1 are varied to determine which parameters maximise the VCN intensity below 1 meV. The VCN intensity obtained at \mathcal{P} , for the optimal combinations of the length of the methane and pH₂ moderator for each radius considered for the combined moderator system, are compared against those obtained for the low-dimensional pH₂ moderator designed for the HBS. The specific procedures implemented for the two parts of this study and corresponding results are described in the following two sections.

In both studies, the tantalum target is defined in the same location and detailed design parameters can be found elsewhere [6]. The distance between the tantalum target and the surface of the water premoderator was set to a distance of 2.7 cm for all simulations. The thickness of the water premoderator between the target and the combined VCN moderator was set to 1.5 cm, as fast neutrons emanating from the tantalum target can be efficiently moderated to thermal energies within \sim 1 cm owing to the high moderation ratio of water. The depth of the water moderator in all other directions around the combined VCN moderator was always set to 10 cm. The surrounding water depth was set to 10 cm to encourage further slowing of undermoderated neutrons and reflection back into the combined moderator geometry. A neutron mask, defined as a -1 region, or particle annihilating region, was placed on the outside of the moderator geometry, as method to restrict the view from the point \mathcal{P} to the

Table 1. A summary of the parameters which were used in the [Source] card to describe the properties of the artificial source are presented.

s-type	2
Projectile	Neutron
e_0 (meV/n)	25
dir	All
x_{\min} (cm)	- 5.0
x_{\max} (cm)	5.0
y_{\min} (cm)	- 10.0
y_{\max} (cm)	10.0
Δz (cm)	0.25

opening of the extraction channel, and hence the combined VCN moderator.

To improve the efficiency of the simulations, the point tally estimator is invoked in PHITS with the [T-Point] card to calculate the flux, Φ at a point \mathcal{P} which was always set at a distance $L = 100$ cm from the exit surface of the extraction channel. Care should be taken to note that the flux, Φ , evaluated with the point tally is reported in units of $\text{n}/\text{cm}^2/\text{pr}$ and we adopt this convention in this paper. Strictly speaking, the proper flux is defined in units of $\text{n}/\text{cm}^2/\text{s}$. The flux per solid angle, \mathcal{B} , can be extracted since the view of \mathcal{P} is restricted to the exit of the extraction channel with the neutron mask. The quantity \mathcal{B} can be estimated from the neutron intensity Φ by the relation,

$$\mathcal{B} = \Phi / \Omega \quad (1)$$

where the solid angle Ω is

$$\Omega = \frac{\pi \cdot R^2}{L^2} \quad (2)$$

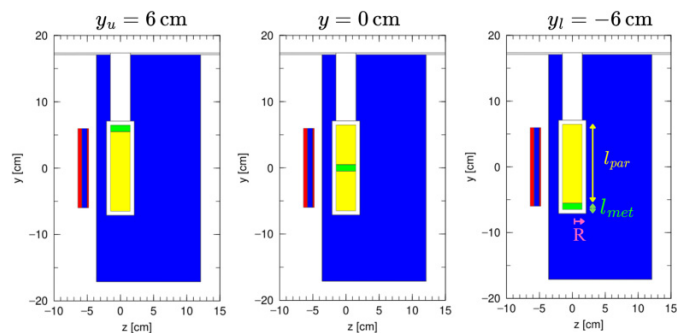
and R represents the radius of the combined VCN moderator/extraction channel. As the quantity \mathcal{B} is proportional to the neutron brilliance, we shall refer to it as the neutron brilliance, henceforth, because it is an indicator of the variation of the neutron brilliance when the performance of the combined moderator geometry is being evaluated. The proper definition of the neutron brilliance can be found in ref. [13]. The JENDL5.0 thermal scattering libraries were utilised for pH_2 at 20 K and methane at 20 K [14].

3. Geometrical optimisation

For the geometrical optimisation calculations, an additional method was implemented to reduce the computation time. An artificial, rectangular monoenergetic thermal neutron source with parameters outlined in Table 1 was embedded in the water premoderator as seen in Fig. 1.

It is appropriate to use an artificial source in lieu of the true source for a few reasons. The first is that fast neutrons coming from the tantalum target are efficiently moderated to thermal neutron energy scales after travelling 1 cm in the

Fig. 2. A plot of three cases of the geometry considered in the study of optimal position of the methane moderator. Selected cases with the methane moderator at the top, middle, and bottom of the tube are illustrated from left to right.



water premoderator by virtue of its high moderation ratio. The artificial source was also deemed an appropriate substitution after comparing the spatial extent of the thermal neutron field it produces in the water premoderator with that which is produced when the fast neutrons from the tantalum target are moderated in the premoderator. The artificial source dimensions produce a thermal neutron cloud with dimensions which reflect most importantly, the extent of the thermal neutron cloud along the \hat{y} direction, from $y = -10$ to $+10$ cm. This detail ensures that the pH_2 portion of the moderator is properly fed along the entirety of its length.

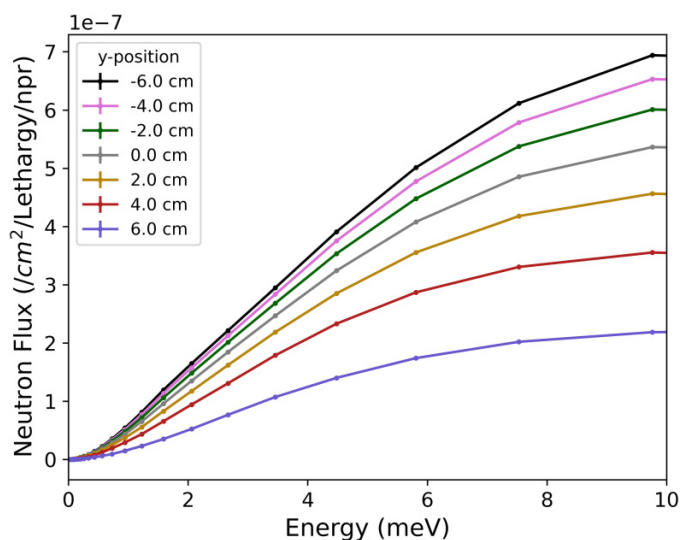
3.1. Vary methane position

In the first part of the optimisation study, where the optimal position, y , of methane within the pH_2 volume was carried out, the combined length of the pH_2 and methane moderator system was fixed to $l = 12$ cm. The length of the methane moderator was set to $l_{\text{meth}} = 1.0$ cm. The position of the methane moderator section was varied from $y_l = -6$ cm to $y_u = +6$ cm in 2 cm steps. y_l and y_u represent the position of the methane disk at the extreme ends of the combined moderator tube, which are furthest and closest from the extraction channel, respectively, as shown in Fig. 2.

Figure 3 shows the neutron spectrum calculated with the point tally estimate for various positions of the methane disk in the combined moderator. The neutron intensity is highest below 1 meV when the methane disk is placed furthest away from the extraction channel. This shows that the extraction depth is the dominating contribution to the performance of the cryogenic moderator. The reduced scattering cross section of pH_2 permits low-energy neutrons to pass straight through a thick layer of the material. The absorption remains low, as the path of the neutron is minimized. If the neutron passes through a layer of methane, the neutron path follows a random walk that is much longer, and hence leads to a stronger absorption. Therefore, the volume below the methane layer contributes only weakly.

The cold neutrons which travel toward the methane moderator also do so unhindered, and can undergo further moderation when they eventually interact with the methane disk and are subsequently scattered back into the pH_2 section of

Fig. 3. The neutron flux ($\text{n}/\text{cm}^2/\text{pr}$) which is obtained at point \mathcal{P} is plotted as a function of neutron energy in meV for the combined moderator geometry in which all parameters, except for the position of the methane disk y , are fixed.



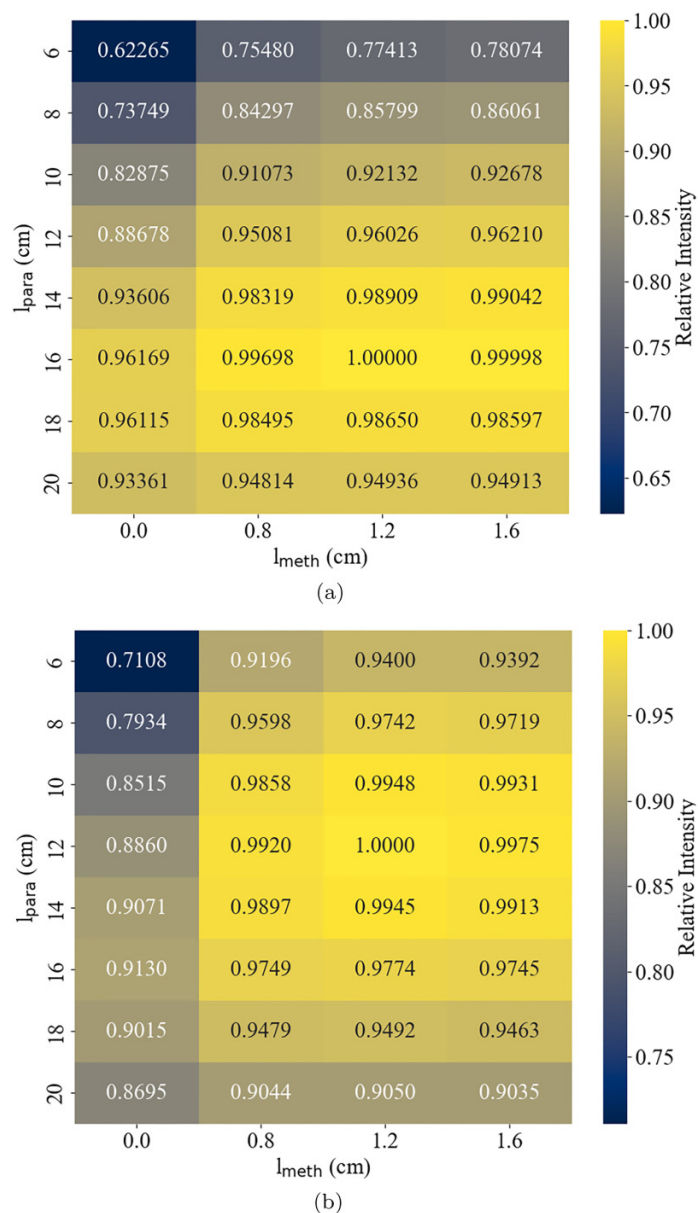
the combined moderator system. As a result, the best position of the methane disk is realised when the entire length of the pH_2 volume is directly fed thermal neutrons for efficient thermal to cold neutron conversion, and methane is placed opposite to the extraction channel, so that it scatters moderated neutrons back into the pH_2 medium, which are subsequently able to travel into the extraction channel without undergoing subsequent interactions in the pH_2 moderator.

3.2. Optimisation of moderator dimensions

As it was determined that the methane disk is best placed at the bottom of the moderator tube, the appropriate optimisation parameters were determined to be the radius of the combined moderator, R , the length of the pH_2 cylinder, l_{para} , and the length of the methane l_{meth} disk as illustrated in right panel of Fig. 2. R was varied from 1.0 to 2.5 cm in 0.5 cm increments, and the case $R = 5.0$ cm was also run to further investigate the effect of increasing the methane- pH_2 contact area. The cylindrical methane moderator height, l_{meth} , was varied from 0.8 to 1.6 cm in 0.4 cm steps, while the height of the pH_2 moderator, l_{para} , was varied from 6 to 20 cm in steps of 2 cm. From this study, the best performing combinations of l_{meth} and l_{para} , with respect to the VCN flux and brilliance obtained at point \mathcal{P} for each moderator radius R case studied were determined. Unsurprisingly, the VCN flux is maximised for geometries where the radius is set to $R = 5.0$ cm, while the VCN brilliance is maximised for the geometries in which the radius is set to 1.0 cm.

We describe the results presented for the optimisation of the VCN flux at point \mathcal{P} as a function of R , l_{meth} , and l_{para} . Each panel presented in Fig. 4 corresponds to the results for a single case R . The x and y axes correspond to the length of the methane disk l_{meth} and the length of the pH_2 mod-

Fig. 4. The relative intensity of the very cold neutron flux, Φ , at point detector position is presented for the cases (a) $R = 1.0$ cm and (b) $R = 5.0$ cm.



erator. The relative intensity values are rescaled by the intensity achieved by the optimal selection of l_{meth} and l_{para} for a given R . From panel (Fig. 4a), or $R = 1.0$ cm case, the VCN flux is observed to increase by a negligible margin, $\sim 4\%$ with the addition of methane at the base of the tube. The increase of the VCN flux when the pH_2 cylinder is increased from 6 to 16 cm is expected for two major reasons. On one hand, increasing the length of pH_2 increases the volume that is populated with cold neutrons from by the pre-moderator, and from which cold neutrons can be extracted without significant absorption. When we consider the $R = 5.0$ cm case as shown in Fig. 4b, similar trends are observed, except the VCN yield increases by 11%. The results are not affected if we plot the brilliance in the same man-

Table 2. A summary of the parameters which were used in the [Source] card to generate the real source characteristics of the triple-layer High Brilliance Source tantalum target are presented.

s-type	2
Projectile	Proton
e_0 (MeV/u)	70
dir	1
x_{\min} (cm)	-5.0
x_{\max} (cm)	5.0
y_{\min} (cm)	-5.0
y_{\max} (cm)	5.0
z_{\min} (cm)	-3.0
z_{\max} (cm)	-3.0

ner, as each dataset would be rescaled by exactly the same value, $\frac{\pi \cdot R^2}{l^2}$.

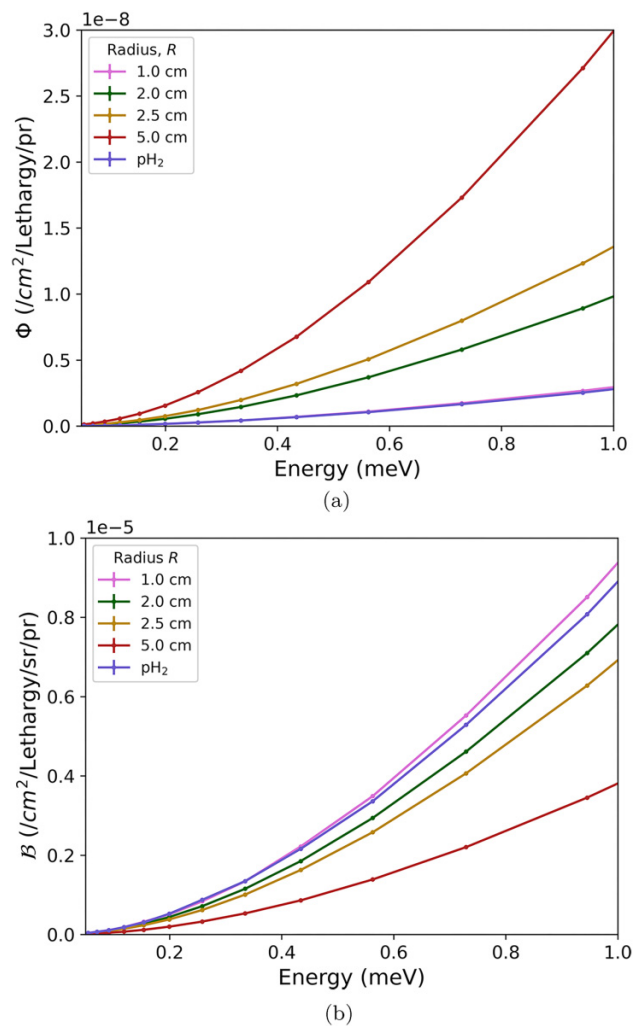
4. Comparison with low-dimensional parahydrogen moderator

For the final part of this study, the performance of the best moderator solutions from the optimisation study are compared against the performance of the low-dimensional pH_2 moderator with respect to the VCN flux and brilliance obtained at point \mathcal{P} . However, additional simulations employing the proper HBS source were run for each optimised geometry obtained for each radius R , and for the low-dimensional HBS pH_2 moderator.

These simulations were performed in a two-step process. The first simulation was conducted to generate a neutron source file that can describe the HBS source characteristics and be utilised for subsequent simulations on a real source. The parameters utilised in the [Source] card in PHITS are summarised in Table 2. A [T-Cross] tally card with dump option was employed in PHITS to record all neutrons exiting the target surface and into the surrounding vacuum region, where it was assumed that any neutron leaving the target surface does not re-enter the target. The dump function writes the 10 variables characterising the neutrons exiting the target into an MCPL file [15], which is later used as the source file. Simulations performed for the optimised geometries and the low-dimensional pH_2 moderator were run using the MCPL source file. The radius and length of the low-dimensional pH_2 moderator were set to $R = 1.0$ cm and $l = 16.0$ cm, respectively.

Figure 5 shows the (a) VCN flux and (b) VCN brilliance plotted as a function of energy, for the optimal combination of parameters obtained for l_{para} and l_{meth} for each radius R considered. The performance of the low-dimensional pH_2 moderator is overplotted in both panels. Table 3 summarizes the cumulative VCN flux and brilliance obtained in each scenario. The $R = 1.0$ cm case shows a negligible improvement in the VCN flux and VCN brilliance over the low-dimensional pH_2 moderator. Figure 5 illustrates that the shape of the neutron spectra are also similar, indicating that the introduction of

Fig. 5. Cross comparison of concept #1 geometries and the cold parahydrogen pencil moderator, with respect to (a) Point tally flux per Lethargy, Φ and (b) Point tally flux per Lethargy per unit solid angle, \mathcal{B} . The radius and length of the low-dimensional pH_2 moderator were selected as $R = 1.0$ cm and $R = 16.0$ cm, respectively.



methane does not significantly reduce the neutron temperature when combined with the parahydrogen moderator. This indicates that the pH_2 moderator volume is the primary contributor to the neutron moderation process in the combined moderator geometry. From Table 3 we note that increasing the radius of the combined moderator from $R = 1.0$ cm to $R = 5.0$ cm leads to a reduction in the VCN brilliance by a factor of 73%. This is expected in the current scenario where pH_2 dominates the cold neutron moderation process. Most of the cold neutron moderation occurs within a small moderator volume because the water premoderator and pH_2 efficiently moderate neutrons coming from the target. While increasing the neutron extraction volume (equivalently, the moderator volume) in geometries with larger radii leads to an improvement in moderation of undermoderated neutrons coming from the target, the VCN cloud in parahydrogen loses phase space density at larger depths, leading to a reduction in the VCN bril-

Table 3. A summary of the cumulative very cold neutron flux and brilliance obtained for each optimal combination of l_{meth} and l_{para} for each R studied.

R	Flux, Φ (n/cm ² /pr)	Relative Error	Ratio $\Phi/\Phi_{\text{pencil}}$	Brilliance, \mathcal{B} (n/cm ² /sr/pr)	Ratio $\mathcal{B}/\mathcal{B}_{\text{pencil}}$
1.0	1.69E-09	0.004	1.04	5.38E-06	1.03
2.0	5.68E-09	0.002	3.48	4.52E-06	0.87
2.5	7.80E-09	0.002	4.79	3.97E-06	0.76
5.0	1.16E-08	0.001	10.31	1.48E-06	0.28
Pencil	1.63E-09	0.004	1.0	5.19E-06	1.0

liance. There is an increase in the total VCN flux by a factor 7 when comparing the low-dimensional pH₂ moderator performance with that of the $R = 5.0$ cm combined moderator geometry, due to the aforementioned increase in moderation volume and in part, due to introduction of methane in the moderator geometry.

5. Conclusion

In this work, a combination methane and pH₂ moderator concept is explored for implementation at the HBS, wherein methane is employed as a VCN converter for neutrons emanating from a cold, liquid pH₂ moderator. It was determined that minimal gains of 4% are realised when the moderator geometry is optimised for brilliance, with $R = 1.0$ cm. However, increased gains of up to 11% are realised in the VCN intensity when the moderator geometry is optimised for overall intensity. The combined moderator spectrum is not significantly shifted from the pure pH₂ case, encouraging the further study of other geometrical concepts for a combined pH₂ and methane geometry. This study importantly points to an important design consideration for methane moderators. Methane would ideally be designed to optimise overall intensity, and therefore, larger surface areas, within the target footprint, should be considered in the future. A next concept for exploration could consider the role of methane as the primary VCN moderator, placed directly behind the target with neutron extraction along the same direction of the impinging proton beam. Beyond methane and pH₂, cross sections for candidate VCN moderator materials at HiCANS facilities are limited. With the recent emergence of open-source tools like NCrystal [16] and the development of test moderator facilities around the world [17], the development of thermal scattering kernels for exotic materials has become more viable. Already, potential candidate advanced cold moderator materials have been proposed [18] and should be explored. Therefore, concerted effort geared toward the study of these materials and search for new materials, and experimental and theoretical work on materials for HiCANS would prove to further advance this field of study.

Acknowledgement

The authors would like to acknowledge fruitful discussions with N. Schmidt, E. Mauerhofer, J. Chen, and D. Shabani.

Article information

History dates

Received: 1 April 2025

Accepted: 12 July 2025

Accepted manuscript online: 31 July 2025

Version of record online: 13 November 2025

Notes

This paper is one of a selection of papers from the 11th International Meeting of the Union for Compact Accelerator-driven Neutron Sources.

Copyright

© 2025 The Authors. This work is licensed under a [Creative Commons Attribution 4.0 International License](#) (CC BY 4.0), which permits unrestricted use, distribution, and reproduction in any medium, provided the original author(s) and source are credited.

Data availability

The PHITS input files and corresponding raw datasets are stored on the JCNS server at the website <https://jcnscloud.fz-juelich.de/>. Requests for data access can be directed to the lead author.

Author information

Author ORCIDs

D.D. Maharaj <https://orcid.org/0000-0002-1697-4833>

P. Zakalek <https://orcid.org/0000-0002-6497-9604>

Author notes

Thomas Gutberlet served as Guest Editor for the collection at the time of manuscript review and acceptance; peer review and editorial decisions regarding this manuscript were handled by another editorial board member.

Author contributions

Conceptualization: DDM, UR, JL, TG, PZ

Data curation: DDM

Formal analysis: DDM, JV, PZ

Funding acquisition: DDM

Investigation: DDM

Methodology: DDM, UR, JL, PZ

Project administration: UR

Supervision: UR, TG, PZ

Validation: UR

Visualization: DDM

Writing – original draft: DDM

Writing – review & editing: DDM, UR, JL, JV, TG, PZ

Competing interests

The authors declare there are no competing interests.

Funding information

The authors would like to acknowledge fruitful discussions with N. Schmidt, E. Mauerhofer, J. Chen, and D. Shabani. The project leading to this publication has received funding from the European Union's Horizon 2020 research and innovation programme under the Marie Skłodowska-Curie grant agreement No. 101034266.

References

1. F. Mezei. *J. Neutron Res.* **24**, 205 (2022). doi:[10.3233/JNR-220012](https://doi.org/10.3233/JNR-220012).
2. J.M. Carpenter and B.J. Micklich. Proceedings of the workshop on applications of a very cold neutron source, technical report ANL-05/42. Argonne National Laboratory. 2005.
3. F.X. Gallmeier, T. Hügler, E.B. Iverson, W. Lu, and I. Remec. *J. Phys. Conf. Ser.* **1021**(1), 012083 (2018). doi:[10.1088/1742-6596/1021/1/012083](https://doi.org/10.1088/1742-6596/1021/1/012083).
4. V. Santoro, et al. *J. Neutron Res.* **25**, 85 (2024).
5. L. Zanini, E. Dian, and D.D. DiJulio, et al. *J. Neutron Res.* **24**, 77 (2022).
6. J. Baggemann, et al. Technical design report HBS volume 2—target stations and moderators, technical report ISBN 978-3-95806-710-3. Forschungszentrum Jülich, 52428 Jülich, Germany. 2020.
7. M. Huerta Parajon, E. Abad, and F.J. Bermejo. *Phys. Procedia*, **60**, 74, 3rd International Meeting of the Union for Compact Accelerator-driven Neutron Sources, UCANS III, 31 July–3 August 2012, Bilbao, Spain & the 4th International Meeting of the Union for Compact Accelerator-driven Neutron Sources, UCANS IV, 23-27 September 2013, Sapporo, Hokkaido, Japan(2014). doi:[10.1016/j.phpro.2014.11.012](https://doi.org/10.1016/j.phpro.2014.11.012).
8. I.I. Gurevich and L.V. Tarasov. Low-energy neutron physics. North-Holland Publishing Co., Amsterdam. 1968.
9. Y. Shin, W. Mike Snow, C.Y. Liu, C.M. Lavelle, and D.V. Baxter. *Nucl. Instrum. Methods Phys. Res. Sect. A*, **620**(2), 382 (2010). doi:[10.1016/j.nima.2010.03.109](https://doi.org/10.1016/j.nima.2010.03.109).
10. K. Inoue, N. Otomo, H. Iwasa, and Y. Kiyanagi. *J. Nucl. Sci. Technol.* **11**, 228 (1974). doi:[10.1080/18811248.1974.9730652](https://doi.org/10.1080/18811248.1974.9730652).
11. H. Iwase, K. Niita, and T. Nakamura. *J. Nucl. Sci. Technol.* **39**, 1142 (2002). doi:[10.1080/18811248.2002.9715305](https://doi.org/10.1080/18811248.2002.9715305).
12. T. Sato, et al. *J. Nucl. Sci. Technol.* **61**, 127 (2024).
13. J. Baggemann, et al. Conceptual design report jülich High Brilliance Neutron Source (HBS), technical report ISBN 978-3-95806-501-7. Forschungszentrum Jülich, 52428 Jülich, Germany. 2020.
14. O. Iwamoto, et al. *J. Nucl. Sci. Technol.* **60**, 1 (2023).
15. T. Kittelmann, et al. *Comput. Phys. Commun.* **218**, 17 (2017).
16. X.-X. Cai and T. Kittelmann. *Comput. Phys. Commun.* **246**, 106851 (2020). doi:[10.1016/j.cpc.2019.07.015](https://doi.org/10.1016/j.cpc.2019.07.015).
17. E.B. Iverson, K.C. Johns, F.X. Gallmeier, and K.B. Grammer. *EPJ Web Conf.* **298**, 05009 (2024). doi:[10.1051/epjconf/202429805009](https://doi.org/10.1051/epjconf/202429805009).
18. J.R. Granada. *J. Neutron Res.* **26**, 144 (2025).